Chemical Engineering Communications
Publication details, including instructions for authors and subscription information:
http://www.tandfonline.com/loi/gcec20

STEADY STATE AND DYNAMIC MODELLING OF A PACKED BED REACTOR FOR THE PARTIAL OXIDATION OF METHANOL TO FORMALDEHYDE II. EXPERIMENTAL RESULTS COMPARED WITH MODEL PREDICTIONS

MARVIN J. SCHWEDOCK [a] , LARRY C. WINDES [a] & W. HARMON RAY [a]
[a] Department of Chemical Engineering , University of Wisconsin , Madison , WI , 53706
Published online: 05 Apr 2007.

To cite this article: MARVIN J. SCHWEDOCK , LARRY C. WINDES & W. HARMON RAY (1989) STEADY STATE AND DYNAMIC MODELLING OF A PACKED BED REACTOR FOR THE PARTIAL OXIDATION OF METHANOL TO FORMALDEHYDE II. EXPERIMENTAL RESULTS COMPARED WITH MODEL PREDICTIONS, Chemical Engineering Communications, 78:1, 45-71, DOI: 10.1080/00986448908940186

To link to this article: http://dx.doi.org/10.1080/00986448908940186

Chem. Eng. Comm. 1989, Vol. 78, pp. 45–71
Reprints available directly from the publisher.
Photocopying permitted by license only.

Printed in the United States of America

STEADY STATE AND DYNAMIC MODELLING OF A PACKED BED REACTOR FOR THE PARTIAL OXIDATION OF METHANOL TO FORMALDEHYDE

II. EXPERIMENTAL RESULTS COMPARED WITH MODEL PREDICTIONS

MARVIN J. SCHWEDOCK,† LARRY C. WINDES,‡
and W. HARMON RAY§

Department of Chemical Engineering
University of Wisconsin
Madison, WI 53706

(*Received September 21, 1987*)

Heterogeneous and pseudohomogeneous two-dimensional models are compared to steady state and dynamic experimental data from a packed bed reactor for the partial oxidation of methanol to formaldehyde over an iron oxide-molybdenum oxide catalyst. Highly effective parameter estimation software was used to fit selected model parameters to large sets of experimental data so as to obtain small residuals. Heat transfer parameters which were successful in matching data from experiments without reaction were not capable of fitting data from experiments with reaction, and it was necessary to increase the radial heat transfer for higher temperatures or reaction rates. Axial composition profile data was represented by estimating the preexponential factors and activation energy in a half-order redox rate expression for methanol oxidation. After some decline in catalyst activity, a time-varying axial catalyst activity profile was determined from the data. A redox-type rate expression for the oxidation of formaldehyde to carbon monoxide was proposed to fit the data. The dynamics of the reactor temperature profile were accurately represented by the model. The heterogeneous and pseudohomogeneous models gave similar results in fitting experimental data, although the parameters determined for the two models were somewhat different.
KEYWORDS Packed bed Oxidation Methanol Formaldehyde.

INTRODUCTION

In this paper experimental results for the catalytic oxidation of methanol in a packed bed reactor are presented and used to improve estimates of parameters in a mathematical model of the reactor presented in Part I (Windes *et al.*, 1988). The resulting model is then compared with a wide range of data from both steady state and dynamic experiments. An important contribution of this work is the accurate measurement of dynamic, two-dimensional temperature profiles and

† Present address: Unocal, Science & Technology, Brea, CA 92621.
‡ Present address: Tennessee Eastman Co., Kingsport, TN 37662.
§ Author to whom correspondence should be addressed.

axial composition profiles in a wall-cooled packed bed reactor of practical interest. Data has been collected for step changes in wall temperature, feed temperature, feed composition, and flowrate. Because of the wide range of operating conditions under which experiments were conducted, a rather complete experimental picture of the steady state and dynamic behavior of this reactor has been obtained. This data has been used to produce a highly detailed model capable of predicting even the most subtle features of the reactor. Both the experimental runs and the resulting model show new and interesting phenomena from the reactor. We believe that the combined experimental/modelling methodology and parameter estimation methods described here can be valuable in studying other types of packed bed tubular reactors.

EXPERIMENTAL METHODS

Description of the Reactor System

The reaction chosen for these studies is the oxidation of methanol to formaldehyde. This reaction is important industrially and presents interesting selectivity problems which can be overcome through good reactor design and control. A commercial catalyst of iron oxide and molybdenum oxide in the shape of hollow cylinders was used. The two principal reactions which occur are:

$$CH_3OH + \tfrac{1}{2}O_2 \dashrightarrow CH_2O + H_2O \qquad (-\Delta H_R^0) = 37.4 \text{ kcal/mol}$$

$$CH_2O + \tfrac{1}{2}O_2 \dashrightarrow CO + H_2O \qquad (-\Delta H_R^0) = 56.5 \text{ kcal/mol}$$

These reactions were carried out in a highly instrumented tubular packed bed reactor described below.

A schematic diagram of the packed bed reactor pilot plant is given in Figure 1. The reactor tube consists of a schedule 40 one-inch (2.66 cm i.d.) stainless steel pipe, which is concentric with a coolant jacket of schedule 10 three-inch (8.89 cm o.d.) stainless steel pipe. Sun Oil 21 heat transfer oil circulates continuously through the annulus between the two pipes to remove the exothermic heat of reaction produced in the reactor tube. The oil circulates at a high rate to provide a uniform wall temperature. The oil temperature is controlled with a 7.5-KW immersion heater which is inserted in the oil loop. Heat for raising the oil temperature during startup is provided both by the immersion heater and by beaded resistance wire which is coiled around the oil loop. The heating and cooling rates at operating temperatures of ~250°C are equalized by partial insulation of the oil loop.

Oxygen is supplied by feeding air to the reactor. The air flow rate is both monitored and controlled with a Tylan electronic mass flow controller. The methanol flow rate is controlled with a Masterflex peristaltic pump with a variable speed drive. The mole fraction methanol in the feed is maintained through measuring the air flow rate and adjusting the pump speed. The two streams meet in a mixing tee where the methanol vaporizes. The methanol-air mixture is brought to desired feed temperature with heat tapes. For safety and data analysis,

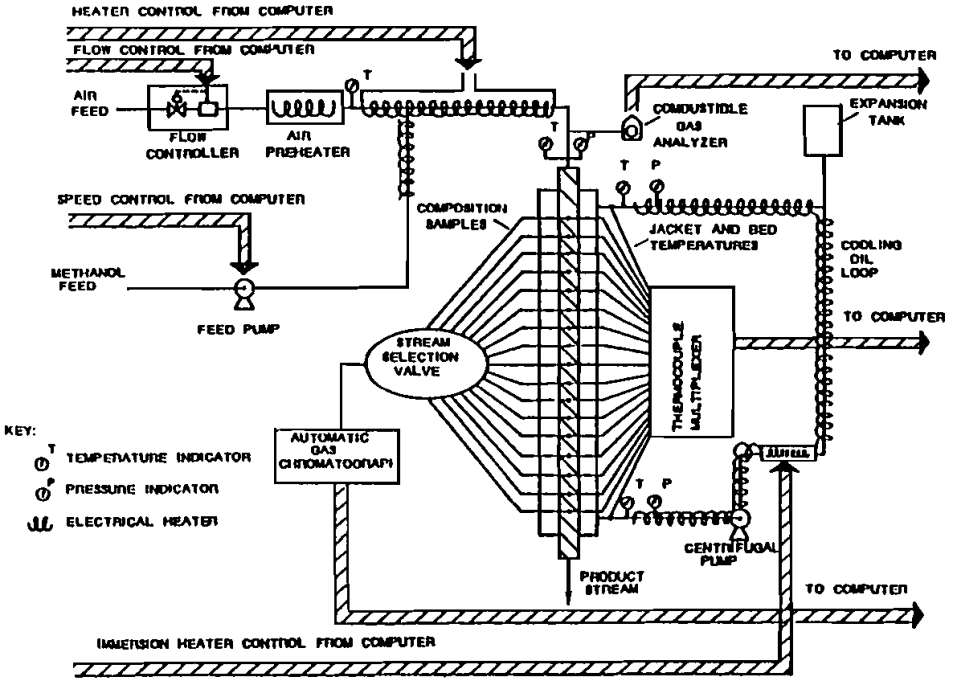

FIGURE 1 Schematic of the packed bed reactor pilot plant.

a Bachrach combustible gas analyzer monitors the methanol fractional composition in the feed stream.

The feed flows down through the catalyst bed, which is 70 cm deep. Sampling ports are located at 5 cm intervals along the entire length of the reactor. The axial composition is measured by taking gas samples from selected ports to a Carle gas chromatograph. The elution time of the chromatograph is approximately 12 minutes so that only steady state composition profiles can be obtained. Three radial temperature measurements are taken at each port by exposed thermocouples permanently positioned at three radial locations: the center-line of the reactor, the wall of the reactor, and half-way between those two points.

The entire pilot plant can be operated either manually or by computer control with a PDP-11/55 minicomputer. The computer is capable of controlling the air flow rate, the methanol flow rate, the feed temperature, the oil temperature, the gas chromatograph valve switching, and the amplifier relay switching. Under either mode of control the computer collects all data coming from the plant. Additionally, an Apple Computer with a color monitor is used as an on-line multipoint graphics recorder for the gas chromatograph, combustible gas analyzer, and any four thermocouples. A more detailed description of the reactor pilot plant is given elsewhere (Schwedock, 1983).

Summary of Experiments

The experiments provide data on the effect of various reactor inputs on the response of the reactor. The experimental operating conditions for the few principal manipulated variables were within the following ranges:

1. Wall temperature—220–270°C
2. Feed temperature—220–290°C
3. Methanol mole fraction in feed—0.01–0.05
4. Total flowrate—0.5–1.4 g/sec

The data consisted of reactor steady state temperature profiles, the transient temperatures between the steady state conditions, and a single composition sample taken every 700 s at one of eight axial locations. A set of 30 temperature measurements was typically made at intervals of 15 s. The temperature measurements were made at 3 radial points in the reactor at each of 10 axial locations:

5, 15, 25, 30, 35, 40, 45, 50, 60, 70 cm.

At each temperature measurement time interval, the output of these 30 thermocouples was recorded in addition to the oil bath and inlet temperature (at $r = 0$, $z = 0$). The wall temperature of the reactor and the coolant oil temperature are assumed to be equal, and all of the wall heat transfer resistance is lumped at the inner wall of the reactor tube.

For most of the experimental runs the wall temperature and inlet temperature were at the same value. Three different feed mole fracions of 0.01, 0.03, and 0.05 were used. The maximum feed mole fraction of 0.05 was established by safety considerations. The four flowrates used in the experiments were: 0.5, 0.7, 1.0, 1.4 g/sec. At the beginning of the catalyst life, the flowrate was 1.4 g/sec. As the catalyst deactivated, the flowrates were decreased and the normal operating temperature increased in order to maintain high conversions. A wide range of steady state and dynamic experiments (with and without reaction) have been used to identify model parameters and to compare reactor performance to model predictions. A complete listing of steady state experiments is given by Windes (1986).

Catalyst Deactivation

An important aspect of reactor operation which was not dealt with in the *a priori* modelling of the reactor is catalyst deactivation. Although the catalyst manufacturer recommended certain procedures in order to provide long catalyst lifetimes, we chose not to use these in our experiments in order to be able to more easily study the phenomena of catalyst deactivation. Thus one observes over a period of weeks and months that reactor conversions and temperatures have gradually decreased for constant reactor inputs. The comparison between run 1 and run 16 for operating conditions $T_w = 260°C$, $y_i = 0.05$, $F = 1.4$ (Shown in Figure 2a) illustrates the drastic change in reactor performance due to partial deactivation of the front part of the catalyst bed. The temperature profiles shift considerably

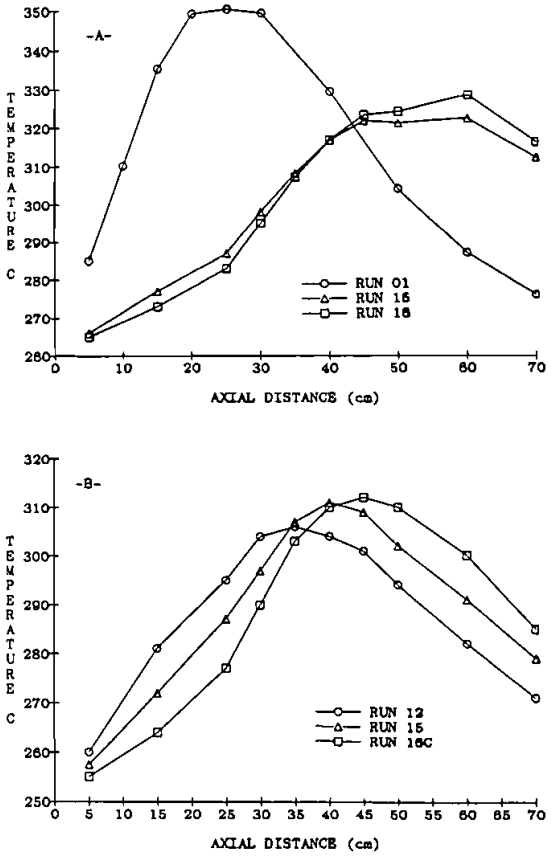

FIGURE 2 Effect of catalyst deactivation on centerline temperature profiles. a. $T_w = T_i = 260°C$, $y_i = 0.05$, $F = 1.4$ g/sec. ○: run #1, △: run #15, □: run #16; b. $T_w = T_i = 250°C$, $y_i = 0.05$, $F = 0.7$ g/sec. ○: run #12, △: run #15, □: run #16c.

toward the exit of the reactor as the catalyst ages. As deactivation occurs, the hot spot temperature can even increase slightly as more reactants are available to the active catalyst in the downstream part of the bed (cf. Figure 2b).

The entire history of the catalyst deactivation has not been followed due to the large numbers of different operating conditions and gaps in the experimental data. In addition, a study of the details and mechanism of the catalyst deactivation is not the purpose of this study. Rather, the goal was to develop a model which could estimate the catalyst activity profile at any time so as to optimize the reactor operation as the catalyst decayed. The techniques for determination of the catalyst activity profile are discussed in the section on parameter optimization.

During the initial operation of the reactor with fresh catalyst, the reactor was at one steady state for long periods of time with negligible catalyst deactivation. However, large changes in reactor performance between run 1 and run 3

indicated much more substantial deactivation than could be predicted by a constant, continuous decline in activity. Low temperature operation with wall temperatures less than 230°C appeared to cause more rapid deactivation. Reactor startup and shutdown did not seem to be detrimental. No increased deactivation was observed during high temperature operation ($T_w \geq 270$°C, maximum temperature less than 370°C). With later runs a slow steady decline in catalyst activity was taking place, and a time varying catalyst activity profile was incorporated into the model for the purposes of fitting the data.

Catalyst deactivation alters the qualitative response of the reactor to changes in the inlet temperature. Increases in the inlet temperature cause increases in the maximum reactor temperature for a constant activity catalyst; however, increases in the inlet temperature cause decreases in the maximum reactor temperature in the presence of partially deactivated catalyst. This behavior is illustrated in Figure 3 for several values of inlet temperature. The changes in the temperature profiles are properly represented by the model with catalyst of much lower activity near the entrance of the reactor. As the inlet temperature increases, the temperatures between 0 and 30 cm increase, but the temperatures downstream of 30 cm decrease. Also, the axial shift in the reactor hotspot with changing inlet temperature is small in comparison to the constant activity catalyst case.

The experiments presented in this paper are divided into three groups:

1. High activity catalyst (initial experiments when catalyst was fresh).
2. Moderate activity catalyst (after some deactivation).
3. Low activity (large number of experiments where activity was monitored as it slowly declined).

The results allow one to see the dramatic influence catalyst deactivation has on reactor behavior.

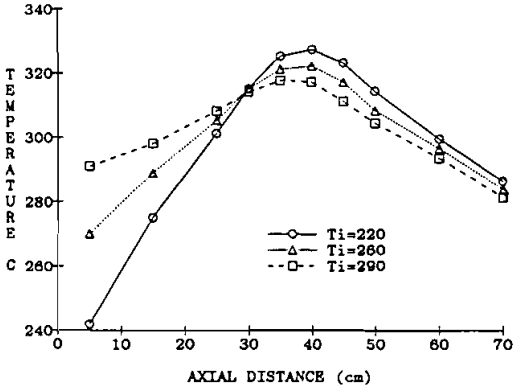

FIGURE 3 Effect of changing inlet temperature on centerline temperature profiles. $T_w = 260$°C, $y_i = 0.05$, $F = 0.7$ g/sec. T_i measured at $z = 0^-$, $r = 0$. ○: $T_i = 220$, △: $T_i = 260$, □: $T_i = 290$.

PARAMETER ESTIMATION METHODS

The model described in Part I (Windes *et al.*, 1988) was used in the present study to fit the experimental data from our reactor by *a priori* choice of most parameters and least squares fitting of a few unknown parameters. The weighted least squares objective function used was:

$$J = \sum_{l=1}^{P} \left(\omega_T \sum_{i=1}^{NZT} \sum_{j=1}^{NRT} \omega_{rj} (T_{ijl} - \hat{T}_{ijl})^2 + \omega_M \sum_{k=1}^{NY} (Y_M - \hat{Y}_M)_{kl}^2 + \omega_C \sum_{k=1}^{NY} (Y_C - \hat{Y}_C)_{kl}^2 \right) \quad (1)$$

where P is the number of experiments in the group; NZT and NRT are number of axial and radial temperature measurements, respectively; NY is the number of composition samples for each experiment; ω_T, ω_{rj}, ω_M, and ω_C are weights.

Initially the least squares computations were carried out using standard numerical optimization packages together with the model simulation. However, this approach was very inefficient and required very long computational times. Thus a new parameter estimation package, GREG (General REGression) developed by Caracotsios and Stewart (cf. Caracotsios, 1986) was applied to the problem. There are two options in the GREG program:

I. Parametric sensitivities are computed by finite differences through repeated evaluation of the objective function. (NP + 2 function evaluations per iteration)
II. Parametric sensitivities are supplied by the user (2 function evaluations per iteration)

The first option can be computationally very taxing; thus a steady state PDE solver PDESAC (Caracotsios, 1986) was used to provide a finite difference solution and parametric sensitivities for the steady state two-dimensional pseudo-homogeneous model. This was continued with GREG-option II to estimate pseudohomogeneous model parameters very efficiently. For the heterogeneous models and for dynamic experiments, the collocation model described in Part I (Windes *et al.*, 1988) was used together with GREG-option I. In this way all of the needed parameters could be estimated from all available data sets and for all types of models.

SELECTION OF MODEL PARAMETERS

There are a number of model parameters that are best adjusted by estimation from experimental data. Although a detailed study has been made of literature correlations for the heat and mass transfer parameters in a packed bed reactor, these correlations are insufficient to accurately describe the reactor behavior, and substantial improvement can be made in the performance of the model by estimating the radial heat transfer from experimental data. Similarly, some kinetic parameters such as the preexponential factor, are dependent on the particular catalyst and must be determined by experiment. Other parameters

have secondary importance and are available from the literature. However, with the wealth of experimental data at hand, it was possible to improve the model by estimating some of these as well. Parameters in this category are activation energies, diffusion limitations of the catalyst, reaction order, flowrate and temperature dependencies of the heat transfer parameters, and the interphase heat transfer coefficient.

Radial Heat Transfer

The radial heat transfer is specified by the Peclet (Pe_{fr}, Pe_{sr}) and Biot (Bi_{wf}, Bi_{ws}) numbers in a two-dimensional reactor model. Only the fluid phase parameters were estimated here because most of the heat is transferred through the fluid phase for this reactor, and Pe_{sr} can be adequately estimated *a priori*. The Peclet and Biot numbers are strongly negatively correlated—decrease in Bi and increases in Pe cause similar changes in the model, especially for the centerline temperature. Therefore, these are reparameterized as $\theta_{Pe} = Pe$ and $\theta_{Bi} = Bi/Pe$, (as suggested by Lerou and Froment, 1978) where θ_{Bi} is now proportional to h_w and does not depend on k_{fr}.

Studies of the temperature and flowrate dependence of the heat transfer parameters show that the Biot number was independent of the wall temperature, but was dependent on the flowrate in the reactor. Also as might be expected, a greater portion of the radial heat transfer resistance occured at the wall in the presence of large flowrates. Results from the parameter estimation for data of run #16 indicated that $\theta_{Bi} \propto F^{-0.5}$. Figure 4 shows the fit of the model to data at the centerline and at the wall at two flowrates. The estimation indicated only a slight dependence of Pe on flowrate at these high Reynolds numbers. A persistent dependence of Pe on the reactor temperature has been found in data from several runs. The radial heat transfer in the reactor is more effective at high temperatures than is predicted for constant Peclet number. Vortmeyer and Winter (1982, 1984) have proposed that the non-idealities in Pe_{fr} are due to non-uniform flow in the packed bed in which the velocity is much more rapid near the wall.

Estimating the non-uniformity in Pe_{hr} from experimental data is a difficult task. A simple correlation of the observed values of Pe_{hr} in terms of reactor temperature and flowrate was found to be:

$$Pe_{hr} = Pe_{hr,0}\left(\frac{F}{F_0}\right)^{\theta_{Pe/F}}(1 + \theta_{Pe/T}(T - T_0)) \tag{2}$$

The results obtained were dependent on both the reactor conditions making up the data and the set of parameters being estimated. This dependence of Pe_{fr} on temperature affects the model's predicted values in a similar manner as decreasing the activation energy or increasing the diffusion limitation in the catalyst (increasing tortuosity). By considering operation at several wall temperatures and by taking numerous composition measurements to provide better estimates of the kinetics, estimated correction factors were found to be:

$$\theta_{Pe/F} = 0.029 \pm 0.025 \qquad \theta_{Pe/T} = -0.0034 \pm 0.0004$$

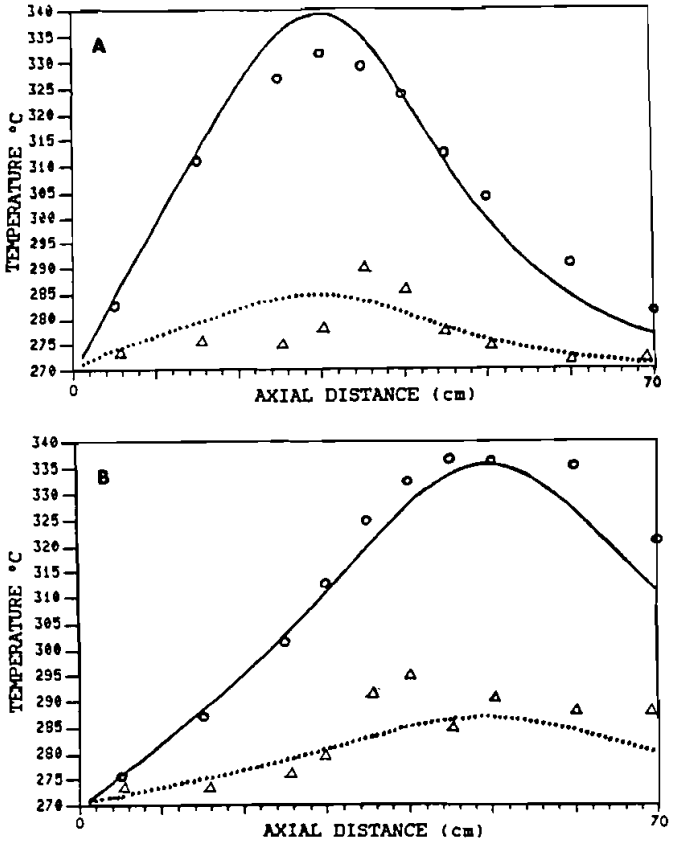

FIGURE 4 Data fitting of centerline and wall temperature profiles using Peclet and Biot number. Data from run #16, $T_w = T_i = 270°C$, $y_i = 0.05$. O—— $r = 0$ (centerline); $\Delta \cdots r = 1$ (wall). a. $F = 0.5$ g/sec. b. $F = 1.4$ g/sec.

Thus the dependence on flowrate is insignificant and with large uncertainty. The parameter $\theta_{Pe/T}$ has only a small uncertainty and has a significant effect.

Kinetics of Methanol Oxidation

The reaction rate expression for methanol oxidation takes the form:

$$R_M = \frac{\eta k_1 p_M^N}{1 + K_a p_M^N} \tag{3}$$

where

$$k_1 = A_1 \exp\{-E_1/R_g T\}$$
$$K_a = A_a \exp\{-E_a/R_g T\} \tag{4}$$

The kinetic parameters (as well as the tortuosity factor, τ) necessary for the

effectiveness factor, η, have been estimated from the data. Estimation of the activation energies E_1, E_a, reaction order N, and adsorption preexponential factor A_a are most effectively estimated for catalyst of uniform activity in the bed. The model is extremely sensitive to changes in the activation energy alone, but is relatively insensitive if A_1 is adjusted so that the reaction rate remains constant at an "average" temperature (usually 280–300°C). An analogous method is used in considering reaction order: A_1 is adjusted so that the reaction rate remains constant at a reference methanol mole fraction (usually $p_M^* = 0.03$). The parameters used in the estimation are:

$$\theta_{A_a} = A_a \exp\left(\frac{-E_a}{R_g T^*}\right) p_M^{*N} \tag{5}$$

$$\theta_{A_1} = A_1 \exp\left(\frac{-E_1}{R_g T^*}\right) \frac{p_M^{*N}}{(1 + \theta_{A_a})} \tag{6}$$

Thus, θ_{A_1} becomes a reaction rate at reference conditions. These parameters were estimated from experiments with fresh catalyst and in conjunction with deactivation parameters in later experiments.

It was not possible to accurately estimate E_a, and it was given its *a priori* value. Accurate determination of the reaction order was also difficult because it was highly correlated with A_a and both parameters inhibit the rate of reaction near the reactor entrance where the concentration of methanol is high. Estimates of the reaction order were in the range 0.5–0.75 depending on the optimized parameter set and the data. A half-order rate expression was chosen with no appreciable increase in the objective function. For fresh catalyst, estimation showed that $A_a \cong 60$, but because this parameter is a ratio of the oxidation and reduction rates, it decreases with catalyst decay. However, in the catalyst deactivation studies, it was difficult to estimate A_a accurately because it reflects the effect of methanol inhibition which is compounded by catalyst deactivation at the entrance of the bed. Therefore, in the runs with large catalyst deactivation, a small value of $A_a = 3$ was selected, and catalyst activity profiles were estimated relative to this value.

For the early reactor experiments the tortuosity factor was estimated to be at or near its lower bound ($\tau = 2$), and optimization of other parameters at a fixed value of $\tau = 4$ resulted in significantly larger model deviation from the data. As hours of reactor operation accumulated, the estimated tortuosity increased. The final estimate was $\tau = 6$–7. This would be consistent with deactivation in the exterior shell of the catalyst particle resulting in a longer diffusion path to the most active sites.

Kinetics of Carbon Monoxide Production

The carbon monoxide production reaction rate is specified by the preexponential factor A_2 and the activation energy E_2. The reaction order was selected to be $N = \frac{1}{2}$. The estimated parameters were transformed in the same way as for the main reaction so that θ_{A_2} (the CO production rate at reference conditions) and E_2

were estimated. Here

$$\theta_{A_2} = A_2 \exp\left(\frac{-E_2}{R_g T^*}\right) \frac{p_F^{*1/2}}{(1 + p_F^{*1/2})} \tag{7}$$

The parameter θ_{A_2} was precisely estimated, but the estimate of E_2 was less reliable. Estimates of E_2 ranged between 10 and 17 kcal/mol, but within this range, E_2 had a small effect on the RMS residual for carbon monoxide.

Catalyst Deactivation

Catalyst deactivation is an important phenomenon to be determined through parameter estimation in order for the model to adequately represent the data. Catalyst activity was assumed to be a function of time and of axial and radial position in the reactor; however, no significant radial dependence of the deactivation was detected from parameter estimates. By contrast, extremely large differences in catalyst activity were found in the axial direction. This decay was represented by a functional form for the preexponential factor A_1:

$$A_1(z) = A_1^+ - (A_1^+ - A_1^0) f_{A_1}(z, Z^0, b_1) \tag{8}$$

The preexponential factor is A_1^0 at the entrance and A_1^+ at the exit. Figure 5 shows the estimated activity profile after 80 hours of reactor operation. The shape of the curve is given by a normalized arctangent function:

$$f_{A_1} = \frac{\tan^{-1}(\alpha(1 - Z^0)) - \tan^{-1}(\alpha(z - Z^0))}{\tan^{-1}(\alpha(1 - Z^0)) - \tan^{-1}(-\alpha Z^0)} \tag{9}$$

where

$$\alpha = \frac{\tan(0.9\pi/2)}{b_1} \tag{10}$$

The inflection point of the curve is at Z^0, and b_1 indicates the steepness of the transition between the regions of low and high activity, while the slope of the

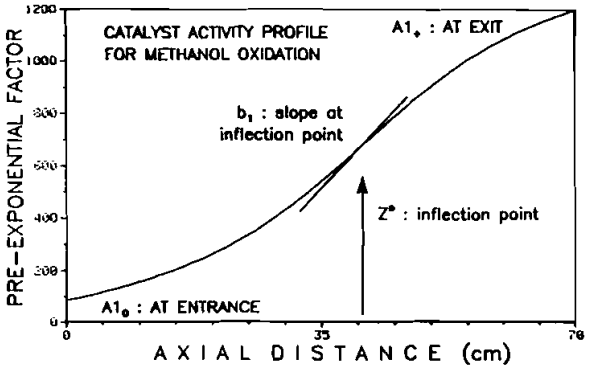

FIGURE 5 Catalyst activity profile for methanol oxidation.

unnormalized arctangent is α at $z = Z^0$. The parameter b_1 is the dimensionless axial distance from the inflection point Z^0 at which the arctangent reaches 90% of its asymptotic value of $\pi/2$. These formulae enable specification of the catalyst activity with the four parameters A_1^+, A_1^0, Z^0, and b_1 which can be functions of time. The parameter b_1 was considered constant, but A_1^+ changed little over the course of the entire experimental program, so that the rate of change of A_1^+ could not be well estimated. However, the time dependence of the parameter A_1^0 was estimated and found to decrease at about 2% per hour.

The activity of the secondary reaction A_2 also decreased with time. Two alternative forms gave equivalent results:

(A) Assuming the same amount of deactivation and shape of deactivation curve as for methanol oxidation, and estimating A_2^+ only, with

$$A_2^0 = A_2^+(A_1^0/A_1^+)$$

(B) Estimating A_2^+ and A_2^0 while assuming a linear deactivation curve:

$$A_2(z) = A_2^+ - (A_2^+ - A_2^0)f_{A_2}(z) = (1 - z)A_2^0 + zA_2^+ \tag{11}$$

By method 2, the activity at the entrance (A_2^0) was estimated to be about 25% of the activity at the exit. The rate of deactivation for $A_2(z)$ was slightly less than for $A_1(z)$, about 1.5% per hour.

Lewis Number

The parameter representing the dynamics of the reactor is the Lewis number (Le) which is the ratio of thermal capacitances (ρC_p) of solid and gas. In the model, Le determines the speed at which the state variables change during integration in time. Since no other parameters have the same role as Le, it was easily estimated from dynamic data.

PARAMETER ESTIMATION RESULTS

Experiments without Reaction

The heat transfer Peclet and Biot numbers were first estimated through experiments without reaction in which the feed air was heated or cooled by the reactor wall. Estimation was performed for the effective heat transfer parameters (Pe_{hr}, Bi_w) in the pseudohomogeneous model and the fluid-phase heat transfer parameters (Pe_{fr}, Bi_{wf}) in the heterogeneous model. For these estimation studies, the solid phase Biot number (Bi_{ws}) was set equal to the fluid phase Biot number (Bi_{wf}) in order to minimize any artifacts of radial interpolation in the collocation solution of the temperature profile. The parameters estimated are given in Table I. The parameters for both models agree well with the correlation given by Dixon and Cresswell, 1979 (discussed by Windes, 1986). There was no discernable difference in the capability of the pseudohomogeneous and heterogeneous models to fit the experimental data. Some example results are shown in Figure 6.

TABLE I

Results of heat transfer parameter estimation from experiments without reaction

	Pe	*Bi*
Heterogeneous Model:		
6 Cooling Experiments	39.16	3.25
3 Heating Experiments	39.09	5.67
All 9 Experiments Together	39.11	3.82
Homogeneous Model:		
6 Cooling Experiments	31.58	3.33
3 Heating Experiments	30.96	5.57
All 9 Experiments Together	31.16	3.82

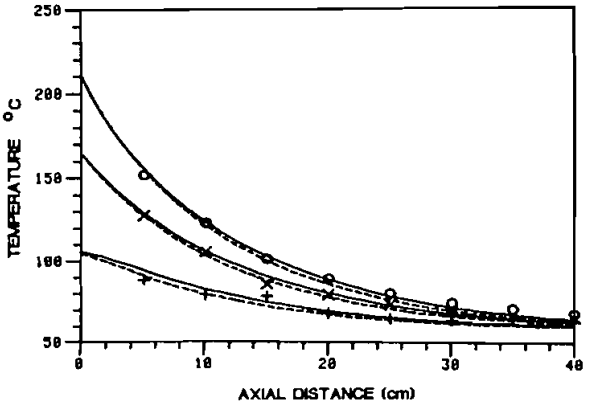

FIGURE 6a Cooling experiment no. 6—heterogeneous simulations. ○: $r = 0$; ×: $r = 0.5$; +: $r = 1$; —— optimal for 6 cooling exp's.; - - - optimal for all 9 exp's.

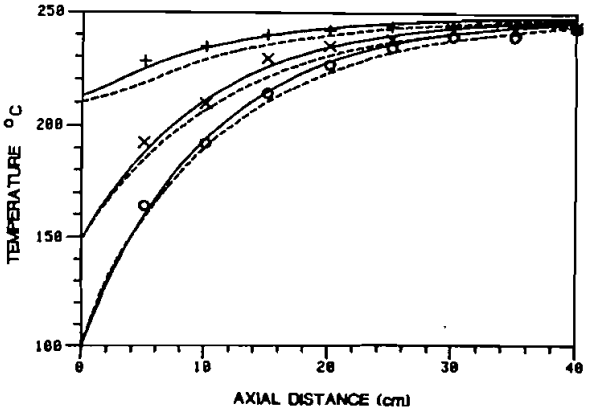

FIGURE 6b Heating experiment no. 3—heterogeneous simulations. ○: $r = 0$; ×: $r = 0.5$; +: $r = 1$; —— optimal for 3 heating exp's.; - - - optimal for all 9 exp's.

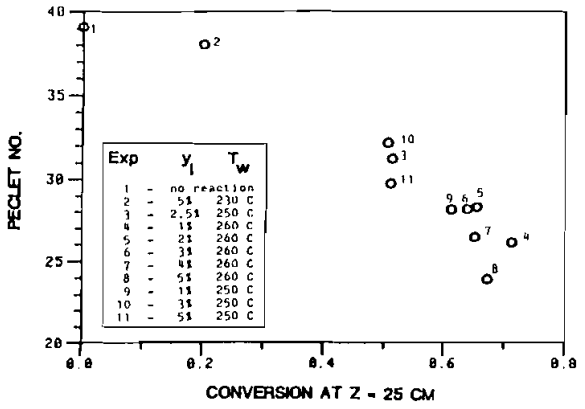

FIGURE 7 Summary of radial Peclet number estimation results for experiments with varying reaction intensity with fresh catalyst.

The significant difference between the Biot numbers for the heating and cooling experiments can be explained by the difference in heat transfer resistance on the oil side of the reactor wall. The oil side heat transfer coefficient is roughly five times greater at the high wall temperatures of the heating experiments than at the low temperatures of the cooling experiments. Therefore the Biot number from the heating experiments has been used as the value representative of reactor operating conditions.

An important finding from our measurement of radial heat transfer under non-reactive conditions is that the value of Peclet number obtained cannot be reliably used to predict reactor performance under reactive conditions. The heat removal from the reactor had to be increased in the model for fast reaction or high temperature conditions. This interaction between heat transfer and reaction rate is not unusual and has been seen by other workers (Paterson and Carberry, 1983; Hofmann, 1979; Panthel, 1977; Hlavacek and Votruba, 1977; Chao, *et al.*, 1973). Therefore, estimation of both heat transfer parameters and kinetic parameters are necessary under reactive conditions. An example of how the estimated radial Peclet number *Pe* varied with "intensity of reaction" is shown in Figure 7. These experiments were with fresh catalyst. Note that radial heat transfer was up to 50% higher at high "reaction intensity" conditions as compared to no reaction.

Steady State Experiments with Fresh (High-Activity) Catalyst

A small number of initial experiments were carried out to obtain a set of steady state axial composition and temperature profiles when the catalyst bed had not deactivated appreciably. These experiments are characterized by relatively high temperatures, high exit conversions, and diffusion limitations within the catalyst within some regions of the reactor. The advantageous feature of this data is that the activity of the catalyst was essentially uniform. The kinetic parameters for methanol oxidation and formaldehyde oxidation as well as Pe_{fr} were determined

TABLE II

Estimated kinetic parameters—high activity catalyst with $E_1 = 19$ kcal/mol, $\tau = 2$

Parameter	Value
A_1	6247
A_2	5.560
A_a	26.82

from this data (Schwedock, 1983). The results are shown in Table II. The resulting model provided a good fit to the experimental data, and some representative results are shown in Figure 8.

Steady State Experiments with Slightly Deactivated Catalyst

This set of experiments was used to determine the kinetic parameters under low reaction rate conditions where catalyst diffusion limitations and the importance of heat transfer parameters are minimized. Unfortunately, these low temperature experiments appeared to cause some deactivation of the catalyst. In fitting this data, the kinetic parameters for methanol oxidation were estimated. The experimental conditions and results are given in Table III, and a representative comparison between the model and data is shown in Figure 9.

Steady State Experiments with Slowly Decaying Catalyst

The later parameter determination experiments attempted to estimate a time-varying activity profile of the catalyst, as discussed above, and to determine the temperature dependency of the radial heat transfer Peclet number. The final parameter estimation consisted of 1198 experimental measurements from 98 steady state experiments. The measurements used were 10 centerline temperatures from each of the 98 experiments, and 109 composition samples each giving a

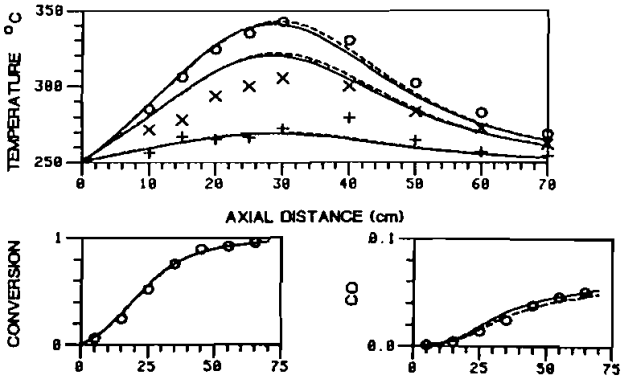

FIGURE 8 Fresh catalyst: $T_f = T_w = 250°C$, $y_i = 5\%$; model comparison (——heterogeneous model, - - - - pseudohomogeneous model). ○: $r = 0$; ×: $r = 0.5$; +: $r = 1$.

TABLE III

Experimental design and estimated kinetic parameters-moderate activity catalyst

Experimental Operating Conditions			
Wall and feed temperature	Mole fraction methanol feed		
	1%	3%	5%
220 C	×	×	×
230 C	×	×	×
240 C	×		×

Feed rate: 1.4 g/sec

Estimated Parameters	
Parameter	Value
E_1	19.00 kcal/mol
A_1	2691
A_a	9.961

value for methanol conversion and carbon monoxide production. Ten parameters for reactor heat transfer and the rate of methanol oxidation were estimated from this data with no indeterminate parameters. Parameters for rate of carbon monoxide production had been estimated from a subset of these experiments, and there was no deterioration in the match between the carbon monoxide measurements and the model prediction. After estimation, the RMS errors in model fit were 2.9°C for temperature, 0.026 for methanol conversion, and 0.005 for carbon monoxide concentration. The computation time for evaluation of each experiment with parametric sensitivity was 26 sec per function evaluation which includes the parameter estimation computations, and the total calculation time was 15100 CPU sec on a VAX-11/785.

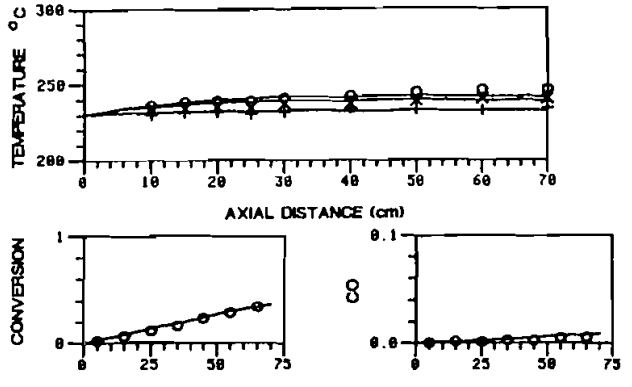

FIGURE 9 Slightly deactivated catalyst: $T_f = T_w = 230$°C, $y_i = 3\%$; heterogeneous simulation. ○: $r = 0$; ×: $r = 0.5$; +: $r = 1$.

TABLE IV

Estimated parameters from 98 steady state experiments

E_1	$\theta^+_{A_1}$	$\theta^0_{A_1}$	$Pe_{hr,0}$	$\theta_{Pe/T}$	Z^0	b_1	dA^0_1/dt	τ	$\theta_{Pe/F}$
Parameter Values:									
18086	26.6	6.88	37.0	−0.0034	0.41	2.0	0.024	6.02	0.029
2-σ Interval (95%):									
433	1.52	0.39	0.52	0.00042	0.019	$1.E+30$	0.002	0.62	0.026
Normalized Covariances of Parameter Estimates:									
1.0									
0.73	1.0								
0.69	0.84	1.0							
−0.33	−0.43	−0.14	1.0						
−0.28	0.18	0.15	−0.032	1.0					
0.23	0.56	0.64	−0.24	0.26	1.0				
0	0	0	0	0	0	0			
−0.21	−0.28	−0.37	−0.061	−0.11	−0.56	0	1.0		
0.76	0.91	0.82	−0.19	0.09	0.27	0	−0.20	1.0	
−0.36	−0.59	−0.53	0.49	−0.17	−0.46	0	0.25	−0.49	1.0
Normalized Test Divisors:									
0.19	0.013	0.069	0.22	0.55	0.048	0.084	0.47	0.013	0.44

The estimated parameters, their 95% highest posterior densities, the normalized covariances of the parameter estimates, and normalized test divisors are given in Table IV. Normalized test divisors less than 0.01 indicate indeterminate parameters. The uncertainty in most of the parameters is small except for $\theta_{Pe/F}$ whose $2-\sigma$ (95%) interval is of the same order as the estimated value. The test divisors are small for $\theta^+_{A_1}$ and tortuosity factor τ indicating difficulty in determining these parameters because of correlation (linear dependence) with the remainder of the parameter set. The covariances were largest between the pairs:

$$\theta^+_{A_1} \leftrightarrow \theta^0_{A_1}; \qquad \theta^+_{A_1} \leftrightarrow \tau; \qquad E_1 \leftrightarrow \tau; \qquad \theta^0_{A_1} \leftrightarrow \tau$$

This off-line parameter estimation procedure gives an impressive fit with such a wide range of data. The values of all parameters for this final fit to the model are given in Table V. Comparisons of this model with experimental data will be illustrated in the next section.

Simplified Model for Process Dynamics and Control

In subsequent papers, we shall describe model-based advanced process control strategies for this reactor. These require a simpler and more computationally efficient model than we have used for representing the steady state behavior. Thus a simplified dynamic model was developed with the following features:

1. No dependence of heat transfer parameters on temperature or flowrate.
2. Most parameters selected *a priori* with a minimal number of fitted parameters.

TABLE V

Summary of model parameters from 98 steady state experiments

Kinetics	
$A_1^+ = 1908$ (mol/s-cm^3 cat-atm$^{1/2}$)	
$A_2^+ = 0.0364$ (mol/s-cm^3 cat-atm$^{1/2}$)	
$A_1^0 = 495$ (mol/s-cm^3 cat-atm$^{1/2}$)	
$A_2^0 = 0.0090$ (mol/s-cm^3 cat-atm$^{1/2}$)	
$Z^0 = 0.414$	$dA_2/dt = 0.014$ per hr.
$b_1 = 2.0$	$dA_1^+/dt = 0.0235$ per hr.
$E_1 = 18010$ (cal/mol)	$dA_1^0/dt = 0$
$E_2 = 10500$ (cal/mol)	$dZ^0/dt = 0$
$A_a = 3.5$	reference time = 62.5 hrs.
$E_a = 2000$	$T^* = 285$ C
$N = 1/2$	$P_M^* = 0.03$
tortuosity, $\tau = 6.0$	$P_F^* = 0.001$
Heat Transfer and Mass Transfer	
$Pe_{hr} = 26.6$	$Pe_{mr} = 20$
$Pe_{fr} = 37.0$	$\theta_{Pe/F} = 0.029$
$Pe_{sr} = 107$ (at $F = 1.0$)	$\theta_{Pe/T} = -0.0034$
$Bi_w = 6.0$	$h_{fs} = 0.025$ (J/cm$^2 - s - K$)

TABLE VI

Simplified dynamic model suitable for process control

Parameters Fixed A Priori:	
Kinetics	
$A_2^+ = 0.0364$ (mol/s-cm^3 cat-atm$^{1/2}$)	
$A_2^0 = 0.091$ (mol/s-cm^3 cat-atm$^{1/2}$)	
$E_1 = 17000$ (cal/mol)	$E_2 = 10500$ (cal/mol)
$A_a = 0$	$b_1 = 2.0$
N (reaction order) = 1/2	
Tortuosity, $\tau = 7.0$	
Heat and Mass Transfer	
$Pe_{sr} = 107$ (at $F = 1.0$ g/sec)	$Bi_{wf} = 6.0$
$Pe_{fz} = 0.4$	$Be_{ws} = 6.0$
$Pe_{sz} = 50$	$Pe_{mr} = 20$
$h_{fs} = 0.025$ (J/cm^2-s-K)	$Pe_{mz} = 2$
$Le = 2300$; $\theta_{Le} = 6.5$	
Parameters Estimated:	
$A_1^+ = 1200 \pm 50$ (mol/s-cm^3 cat-atm$^{1/2}$)	$A_1^0 = 86 \pm 8$ (mol/s-cm^3 cat-atm$^{1/2}$)
$Z^0 = 0.584 \pm 0.017$	$Pe_{fr} = 32.3 \pm 0.8$

Model Fit:

Variable	*RMS Residual*
temperature	3.8 C
methanol conversion	0.025
CO produced	0.005

3. A two-dimensional heterogeneous model formulation, with estimation of 4 parameters using GREG-option I and a small set of dynamic and steady state experiments.

The parameter estimation results are given in Table VI. Note that the principal changes in parameters from Table V are the catalyst activity profile parameters and interacting kinetic parameters; the other parameters are essentially the same. For the simplified dynamic model, the composition predictions are almost as good as the more complete steady state model, but the temperature profile fit is slightly worse. Detailed comparisons with dynamic data will be shown in the next section.

REACTOR MODEL COMPARED WITH EXPERIMENTAL DATA

Steady State Data

The "final" model obtained by estimating parameters from a large amount of data can be compared to steady state experimental data. The centerline temperature profiles calculated by the model are compared with the 10 centerline temperature measurements at each steady state. The axial composition profiles at the wall of the reactor are compared with the measurements of methanol conversion and carbon monoxide production. To facilitate understanding the trends in the data, cases for several values of wall temperature or flowrate are presented on the same graph with all other inputs held constant. Examples of model predictions and data for 5% methanol feed are presented at varying flowrates and wall temperatures in Figures 10–14. Recall that the number of axial composition measurements is limited because of the long elution time of the gas chromatograph.

The model simulation is generally an excellent match with the data. The chief points of discrepancy in the model are:

1. The model tends to predict too close an approach to complete conversion, and the predicted temperatures, conversion, and carbon monoxide production tend to be excessive at higher temperatures.
2. The model is somewhat sensitive at low flowrates.
3. At high flowrates, the predicted hotspot in the downstream section of the reactor is too low.

However, overall the model does an excellent job of representing the data over a wide range of conditions. An important part of the performance of the reactor model is how accurately it matches the exit compositions of the reactor. In Figures 15–16, the measured and predicted methanol conversion and carbon monoxide production are shown as a function of the flowrate and wall temperature.

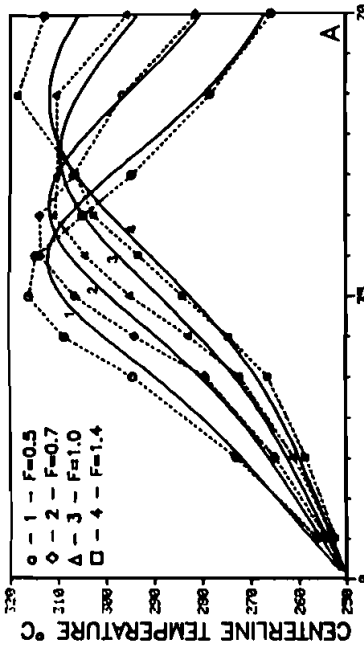

FIGURE 10 Comparison between model and data at steady state. $T_w = 250°C$, $y_i = 0.05$.

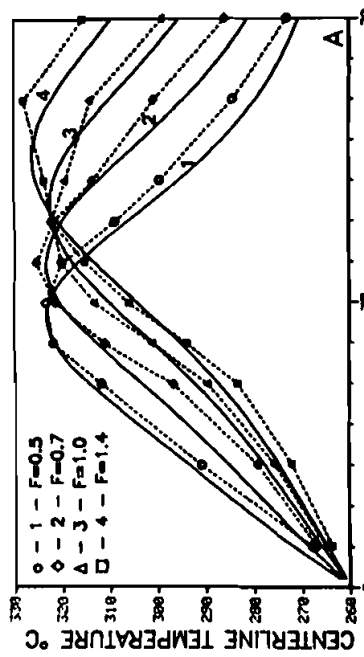

FIGURE 11 Comparison between model and data at steady state. $T_w = 260°C$, $y_i = 0.05$.

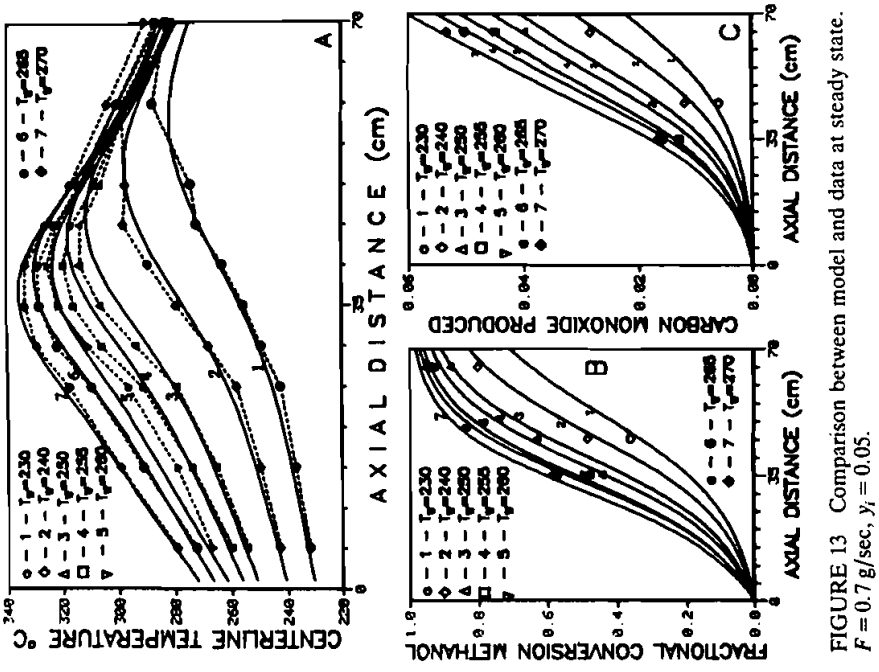

FIGURE 13 Comparison between model and data at steady state. $F = 0.7$ g/sec, $y_i = 0.05$.

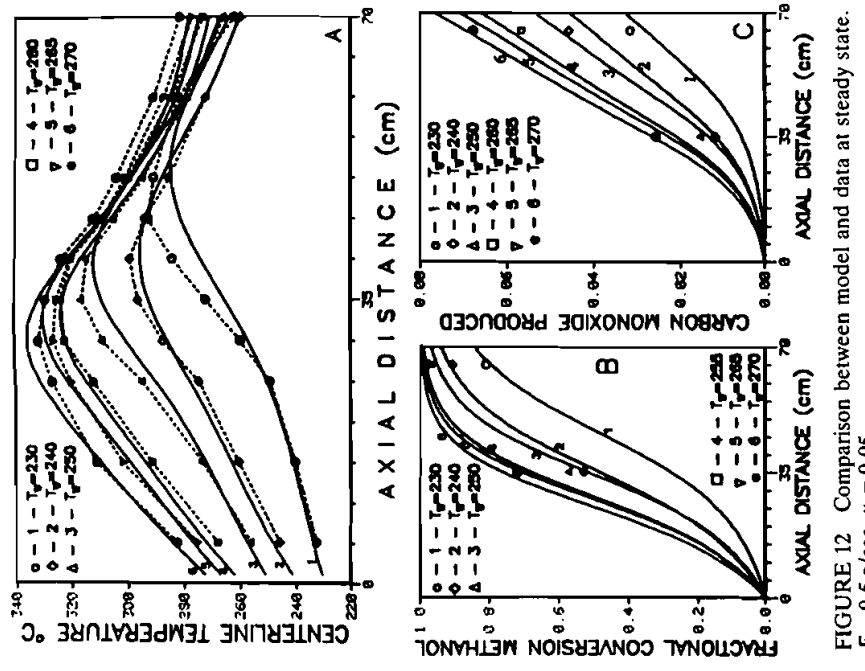

FIGURE 12 Comparison between model and data at steady state. $F = 0.5$ g/sec, $y_i = 0.05$.

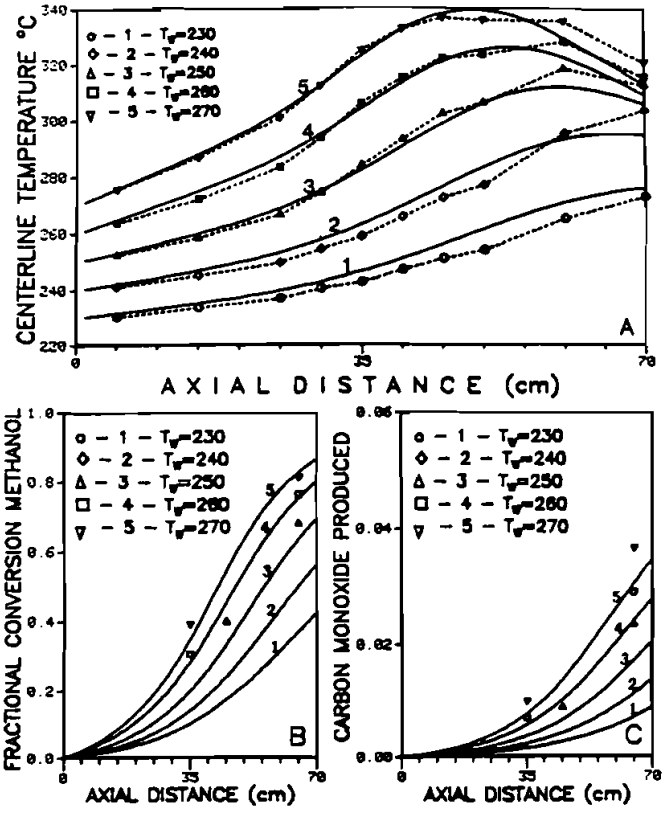

FIGURE 14 Comparison between model and data at steady state. $F = 1.4$ g/sec, $y_i = 0.05$.

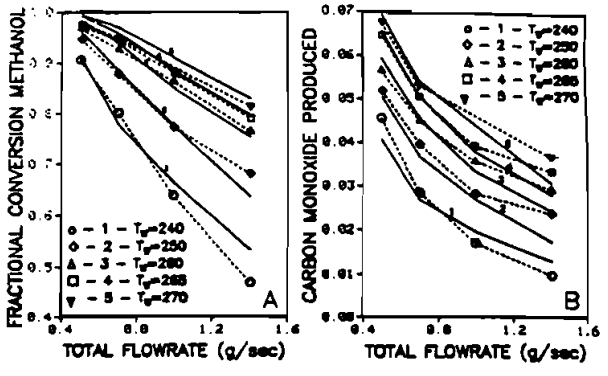

FIGURE 15 Comparison between model and data—exit compositions at steady state as a function of total flowrate. $T_i = T_w$, $y_i = 0.05$. Based on runs 12, 13, 15, 16.

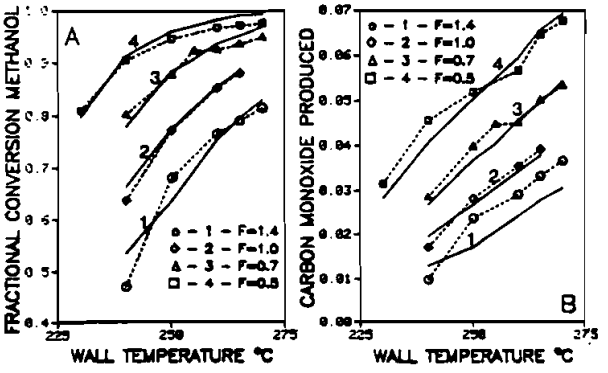

FIGURE 16 Comparison between model and data—exit compositions at steady state as a function of wall temperature. $T_i = T_w$, $y_i = 0.05$. Based on runs 12, 13, 15, 16.

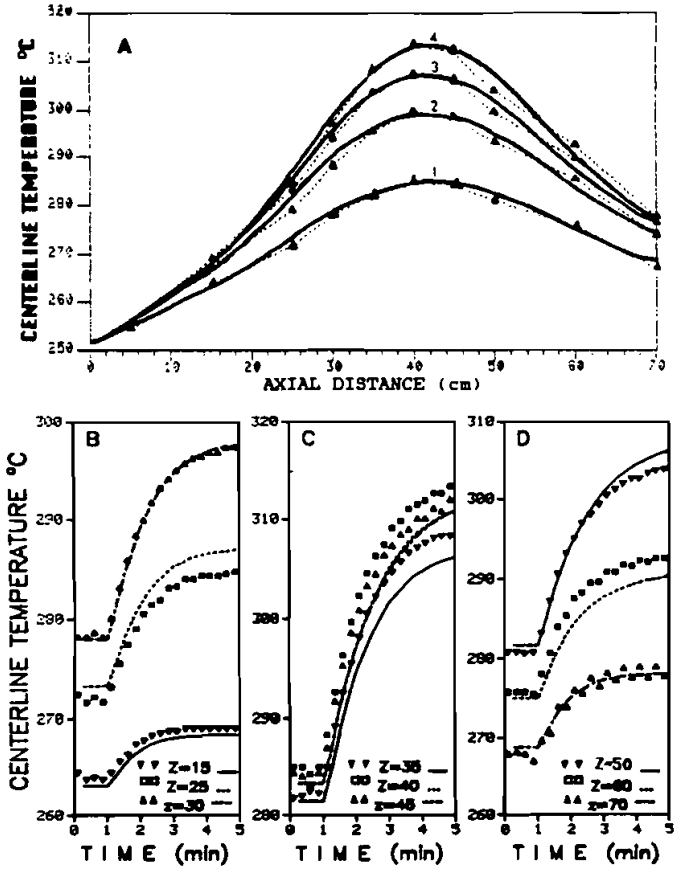

FIGURE 17 Reactor dynamics—comparison between model and data. $T_w = T_i = 250°C$, $F = 0.7$ g/sec. Initial steady state: $Y_i = 0.03$. Final steady state: $Y_i = 0.05$. a. $\Delta \cdots \Delta$ data; —— model. 1: *SS*#1, 2: 1 min, 3: 2 min, 4: 5 min. b. Temperature dynamics at measurement locations.

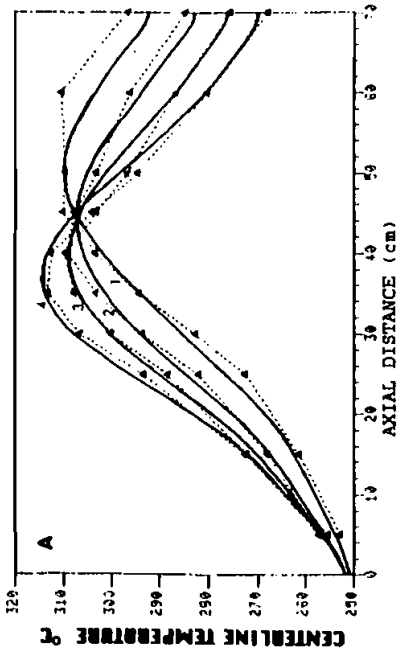

FIGURE 18 Reactor dynamics—comparison between model and data. $T_w = T_i = 250°C$, $Y_i = 0.05$. Initial steady state: $F = 1.0$ g/sec. Final steady state: $F = 0.5$ g/sec. a. $\Delta \cdots \Delta$ data; —— model. 1: SS#1, 2: 1 min, 3: 2 min, 4: 5 min. b. Temperature dynamics at measurement locations.

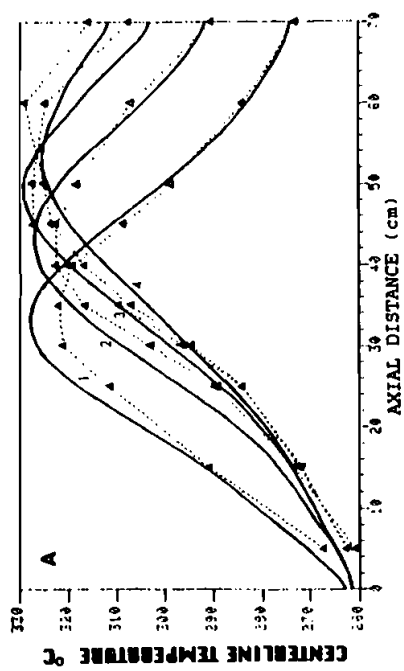

FIGURE 19 Reactor dynamics—comparison between model and data. $T_w = T_i = 260°C$, $Y_i = 0.05$. Initial steady state: $F = 0.5$ g/sec. Final steady state: $F = 1.4$ g/sec. a. $\Delta \cdots \Delta$ data; —— model. 1: SS#1, 2: 1 min, 3: 2 min, 4: 5 min. b. Temperature dynamics at measurement locations.

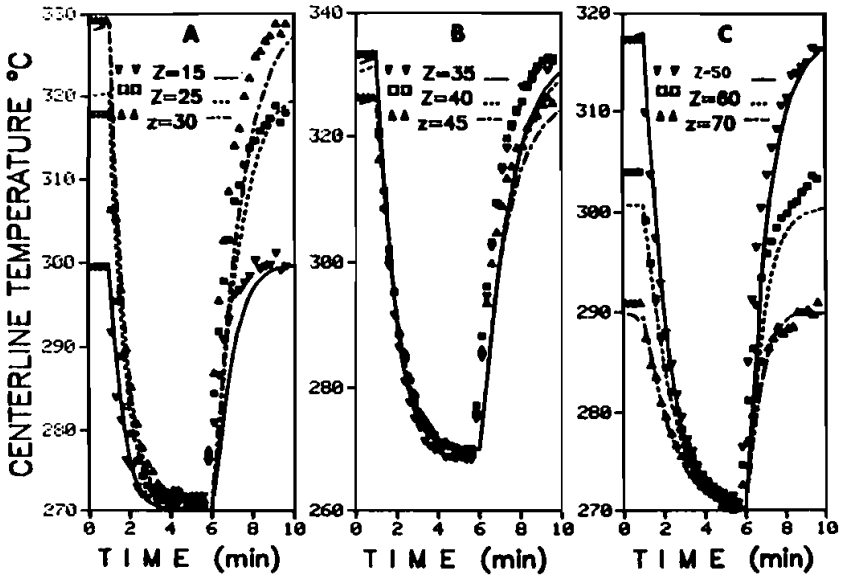

FIGURE 20 Dynamics of temporary reactor shutdown—comparison between model and data. $T_w = T_i = 270°C$, $Y_i = 0.05$, $F = 0.7$ g/sec. 1 min: methanol off; 6 min: ethanol on.

Dynamic Data

The simplified dynamic two-dimensional heterogeneous model discussed above may be compared with dynamic data from the reactor. For each case the reactor begins at steady state and then undergoes a change in the operating conditions. Cases shown in Figures 17–21 include a feed mole fraction increase (Figure 17), a feed flowrate decrease (Figure 18), a large feed flowrate increase (Figure 19), and a shutdown of methonal feed followed by resumption after 5 min. (Figure 20–21).

The dynamic model gave excellent agreement with dynamic data from the reactor. These dynamics were particularly complicated for flowrate changes. For these cases the reactor temperature often showed wrong-way or overshoot behavior in the central regions of the reactor, and the model gave matching results. At either end of the reactor the responses were more monotonic, and the model correctly matched their speed and magnitude. For higher flowrates, the reactor dynamics were much faster than for low flowrates. The model also accurately represented the rate of change in the reactor during startup and shutdown for which the whole temperature profile moved rather uniformly up or down. Thus the dynamic model provided a good basis for later process control studies.

CONCLUDING REMARKS

A comprehensive study of a packed bed reactor for the oxidation of methanol has been carried out. A large amount of high-quality steady state and dynamic

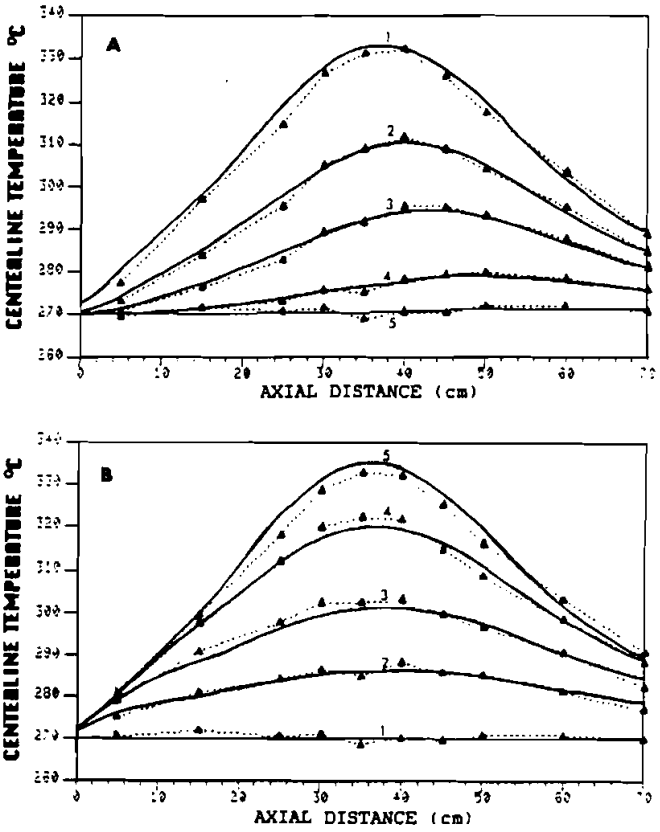

FIGURE 21 Dynamics of temporary reactor shutdown—comparison between model and data. $T_w = T_i = 270°C$, $Y_i = 0.05$, $F = 0.7$ g/sec. 1 min: methanol off; 6 min: methanol on. $\Delta \cdots \Delta$ data; —— model. a. Time elapsed after shutdown: 1: SS#1, 2: 30 sec, 3: 1 min, 4: 2 min, 5: 4 min. b. Time elapsed after startup: 1: SS#2, 2: 30 sec, 3: 1 min, 4: 2 min, 5: 4 min.

experimental data from the reactor are reported. These include a large number of temperature measurements taken simultaneously during transients, composition measurements at several axial locations under steady state conditions, and data spanning a wide range of reactor operating conditions. Several comprehensive non-sequential nonlinear parameter estimation schemes were used together with sophisticated steady state and dynamic models to efficiently determine model parameters. With proper selection of parameters to be estimated, the estimation scheme performed consistently with a small number of iterations and with good robustness to poor initial guesses.

The kinetic parameters found (e.g., an activation energy of 17–19 kcal/mol and a half-order power in methanol for the kinetics of methanol oxidation) are consistent with the work of other workers. However, we found that a redox rate expression was needed for the kinetics of carbon monoxide production. Our heat transfer studies showed clearly that it was not possible to match reactor data *with reaction* with radial Peclet numbers obtained in *non-reactive* heat transfer

experiments. For our modelling, it was necessary to allow Pe_{fr} to be a function of reactor temperature. This phenomenon still requires fundamental quantitative explanation. The reactor exhibited significant catalyst deactivation which greatly increased the effort required in parameter estimation. A time-dependent axial activity profile was identified in order to deal with catalyst deactivation.

After identification of the kinetic parameters, catalyst activity profile, and radial heat transfer in the reactor, the resulting model was compared with the data. The excellent agreement between model and experiment indicates the viability of the mathematical model and the reliability of the estimated parameters. This work is distinctive in that large numbers of experiments were correctly modelled with the same set of parameters. The heterogeneous and pseudohomogeneous models gave approximately the same residuals for this data.

ACKNOWLEDGEMENTS

The authors are indebted to the National Science Foundation, the Department of Energy (Contract No. DE-AC02-80ER 10645.A00), and the DuPont Co. for support of this research.

REFERENCES

Caracotsios, M., "Model Parametric Sensitivity Analysis and Nonlinear Parameter Estimation. Theory and Applications", Ph.D. Thesis, Chemical Engineering Department, University of Wisconsin-Madison (1986).

Chao, R.E., Caban, R.A., and Irizarry, M.M., *Can. J. Chem. Eng.*, **51,** 67–70 (1973).

Dixon, A.G., and Cresswell, D.L., *AIChE J.*, **25** (4) 663–676 (1979).

Hlavacek, V., and Votruba, J., *Chem. Reactor Theory* Ch. 6, N. R. Amundson; L. Lapidus, eds., Prentice-Hall: Englewood Cliffs, New Jersey, 1977.

Hofmann, H., *Ger. Chem. Eng.*, **2,** 258–267 (1979).

Lerou, J.J., and Froment, G.F., *Chem. Eng. J.*, **15,** 233–237 (1978).

Panthel, G., Thesis, Universitat Erlangen, Nurnberg, 1977.

Paterson, W.R., and Carberry, J.J., *Chem. Eng. Sci.*, **38,** 175–180 (1983).

Schwedock, M.J., "Modelling and Identification of a Catalytic Packed Bed Reactor", Ph.D. Thesis, University of Wisconsin (1983).

Schwedock, M.J., Windes, L.C., and Ray, W.H. "Steady State and Dynamic Modelling of a Packed Bed Reactor for the Partial Oxidation of Methanol to Formaldehyde—Experimental Results Compared with Model Predictions", paper 52a, Annual AIChE Meeting, Chicago, November 10–15 (1985).

Vortmeyer, D., and Winter, R.P. "Impact of Porosity and Velocity Distribution on the Theoretical Prediction of Fixed-Bed Chemical Reactor Performance—Comparison with Experimental Data", 7th Int. Symp. Chem. React. Eng., Boston, *ACS Symp. Ser.*, **196,** paper 5, 49–61 (1982).

Vortmeyer, D., and Winter, R.P. "Improvements in Reactor Analysis Incorporating Porosity and Velocity Profiles", *Germ. Chem. Eng.*, **7,** 19–25 (1984).

Windes, L.C. "Modelling and Control of a Packed Bed Reactor", Ph.D. Thesis, University of Wisconsin (1986).

Windes, L.C., Schwedock, M.J., and Ray, W. H., *Chem. Eng. Comm.* see Part I.